Available online at www.sciencedirect.com
ScienceDirect
Journal of Solid State Chemistry 180 (2007) 233–239
JOURNAL OF SOLID STATE CHEMISTRY
www.elsevier.com/locate/jssc

Low-temperature flux syntheses and characterizations of two 1-D anhydrous borophosphates: $Na_3B_6PO_{13}$ and $Na_3BP_2O_8$

Ding-Bang Xiong[a,b], Hao-Hong Chen[a], Xin-Xin Yang[a], Jing-Tai Zhao[a,*]

[a]*The State Key Laboratory of High Performance Ceramics and Superfine Microstructure, Shanghai Institute of Ceramics, Chinese Academy of Science, Shanghai 200050, China*
[b]*Graduate School of Chinese Academy of Science, Beijing, PR China*

Received 19 July 2006; received in revised form 13 September 2006; accepted 14 September 2006
Available online 10 October 2006

Abstract

Two new anhydrous sodium borophosphates with one-dimensional structure, $Na_3B_6PO_{13}$ **(1)** and $Na_3BP_2O_8$ **(2)**, were synthesized by low-temperature molten salts techniques using boric acid and sodium dihydrogen phosphate as flux, respectively. The crystal structures were solved by means of single-crystal X-ray diffraction (**1**, orthorhombic, *Pnma* (no. 62), $a = 9.3727(4)$ Å, $b = 16.2307(7)$ Å, $c = 6.7232(3)$ Å, $Z = 4$; 2 , monoclinic, $C2/c$ (no. 15), $a = 12.567(4)$ Å, $b = 10.290(3)$ Å, $c = 10.210(3)$ Å, $\beta = 92.492(5)^\circ$, $Z = 8$). Compound **1** is characterized by an infinite chain of $^1_\infty\{[B_6PO_{13}]\}^{3-}$ containing eight-membered rings in which all vertexes of borate groups contribute to interconnection. Compound **2** reveals an infinite straight chain $^1_\infty\{[BP_2O_8]\}^{3-}$ built of vertex-sharing four-membered rings, and chains in neighboring layers arranged along different orientations. The relations between structures and the synthetic conditions with only traced water are discussed.

Keywords: Crystal structure; Borophosphate; Flux synthesis

1. Introduction

Since systematic investigations on borophosphates started 10 years ago, a remarkable number of borophosphates containing complex anionic partial structures ranging from isolated species, oligomers, rings, chains, layers to three-dimensional (3-D) frameworks have been reported up to now [1]. Systematic treatments of the borophosphate structural chemistry have also been approached based on the classifications of anionic partial structures, anhydrous and hydrated phases and the (molar) B:P ratios [2,3]. In the systems M_2O–B_2O_3–P_2O_5($-H_2O$) (M = Li, Na, K, Rb, Cs) [4], the ratio of condensed borate and phosphate units in the anions (B:P) covers wide range between 6:1 and 1:3 and eight different ratios exist to date, and Kniep et al. [4a] given a comprehensive introduction to the system in their recent work. There are three predominant common structural features in this group. Firstly, the dimensionality of the anionic partial structures of borophosphates is mostly chain with the exception of 3-D $M^I[B_2P_2O_8(OH)]$ (M^I = Rb and Cs) [4c] and layered $Na_2[BP_2O_7(OH)]$ [4g]. Secondly, all known chains reveal 3-ring motifs except $K_3[BP_3O_9(OH)_3]$ [4a] with open branched chain structure. The chains built exclusively of four-membered rings of borate and phosphate tetrahedra, as present in the structures of $Cs(ZnBP_2O_8)$ [1e] and $NH_4(Zn_{0.88}Co_{0.12}BP_2O_8)$ [5] (B:P = 1:2, straight chain) or in the $(C_4N_3H_{16})[Zn_3B_3P_6O_{24}]\cdot H_2O$ [1d] and $M^IM^{II}(H_2O)_2[BP_2O_8]\cdot H_2O$ (M^I = Li, Na, K, NH_4; M^{II} = Mg, Mn, Fe, Co, Ni, Zn, Cd) [1i,1j] (B:P = 1:2, helical chain), have not been observed in the group of alkali metal borophosphates. Thirdly, all alkali borophosphates but $Na_5[B_2P_3O_{13}]$ [4e] are hydrated phases. Moreover, among all borophosphates prepared hydrothermal method, anhydrous phases are rare.

In the early years of study, borophosphates were mostly obtained through high-temperature solid-state reactions and the systems were very limited. In the middle of 1990s, hydrothermal method was introduced into the syntheses of

*Corresponding author. Fax: +86 021 52413122.
E-mail address: jtzhao@mail.sic.ac.cn (J.-T. Zhao).

0022-4596/$ - see front matter © 2006 Elsevier Inc. All rights reserved.
doi:10.1016/j.jssc.2006.09.034

borophosphates and the number of compounds has grown steadily ever since. Solvothermal method has also been developed recently [4a]. Recently, Lu et al. [6a], Ju et al. [6], Li et al. [6c–e], Williams et al. [7a] and Sung et al. [7b] employed the boric acid flux method for the syntheses of polyborates compounds, in which excess melt boric acid acts as both reaction medium and reactant. In our group, we applied this method to the syntheses of new borophosphates for the first time, and successfully synthesized an ammonium fluorinated borophosphate NH_4BPO_4F with GIS zeolite topology [8a] and a 1-D copper chlorophosphate [8b]. After then, Yang et al. [9] also synthesized two metalloborophosphates with ANA zeolite type topology by using the boric acid flux method.

Here, we report the syntheses and characterizations of two new anhydrous sodium borophosphates, $Na_3B_6PO_{13}$ **(1)** with the highest borate content (B:P = 6:1) observed to date and $Na_3BP_2O_8$ **(2)** with relative high phosphate content (B:P = 1:2), synthesized by using boric acid and sodium dihydrogen phosphate as flux, respectively. The relations between structural features and synthetic conditions are discussed.

2. Experimental section

2.1. Synthesis

Both title compounds were prepared via low-temperature molten salt technique in Teflon-lined stainless-steel autoclaves ($V = 50$ mL) using boric acid or sodium dihydrogen phosphate as flux with a filling degree of 20–30% by the initial powder reactants. The reactants were homogenized by grinding before they were placed into autoclaves. After a reaction time of typically 3 days at 533 K, the autoclaves were removed from the furnace and allowed to cool to room temperature. The final product containing large single crystals were washed with hot water (323 K) until the residual flux and other products in the form of powder were completely removed, and then dried in air at 333 K for further characterizations.

Compound **1** was synthesized from mixtures of 5.600 g H_3BO_3, 1.190 g NaH_2PO_4, 0.420 g NaF and 0.530 g Na_2CO_3 in a molar ratio of 18:2:2:1. The weight percentage composition of elements in $Na_3B_6PO_{13}$ (372.8): calcd. (%) Na 18.49, B 17.38, P 8.31; found (%) Na 16.12, B 16.45, P 7.93.

Compound **2** was synthesized from mixtures of 0.650 g $La[B_8O_{11}(OH)_5]$ (obtained by the reaction of La_2O_3 and H_3BO_3 according to the method described in reference [6d] and 3.570 g NaH_2PO_4 in a molar ration of 1: 23. The reaction of H_3BO_3, NaH_2PO_4, NaF and Na_2CO_3 in the molar ratio of 4:12:2:1 also resulted to compound **2** but with much lower yield. Therefore, the lanthanum compound acted as a sort of catalyst in the reaction. The weight percentage composition of elements in $Na_3BP_2O_8$ (269.7): calcd. (%) Na 25.55, B 4.08, P 22.99; found (%) Na 26.12, B 4.45, P 21.43.

2.2. Other characterizations

The reaction products were examined also by powder X-ray diffraction (Rigaku D/max 2550 V diffractometer, Cu$K\alpha$) to confirm their phase identity and purity. The diffraction patterns were consistent with those calculated from the structures determined by single-crystal X-ray diffraction, which provides evidence of no crystalline impurities for both compounds. Variable-temperature X-ray powder diffraction measurements for **1** were performed using Bruker D8 ADVANCE equipped with high-temperature device (Cu$K\alpha$, temperature steps of 100 K from 300 to 1073 K were used). Thermogravimetric analyses (TGA) were performed using STA-409PC/4/H LUXX DSC-TGA at a heating rate of 10 K min^{-1} in air to a maximum temperature of 1123 K. IR spectra were collected on a Digilab-FTS-80 spectrophotometer using pressed KBr pellets of the samples in the range of 400–4000 cm^{-1}. The elemental analyses were performed with an ICP–AES (Vista AX ICP–AES) instrument.

2.3. Single-crystal structure determination

Colorless single crystals of compound **1** ($0.36 \times 0.16 \times 0.10\,mm^3$) and **2** ($0.10 \times 0.09 \times 0.09\,mm^3$) were selected under a polarizing microscope, glued to a thin glass fiber with cyanoacrylate (superglue) adhesive, and inspected for singularity. Data sets were collected on a Nonius Kappa CCD diffractometer (Mo$K\alpha$ radiation, $\lambda = 0.71073$ Å) at 293(2) K. The data were corrected for absorption using the SADABS program [10a,10b]. All atoms in two compounds were obtained initially by direct method, and then refined against $|F^2|$ with the SHELXTL-PLUS package [10c]. Additional information about the data collections and structure refinements are presented in Table 1, and selected distances and angles for **1** and **2** are listed in Tables 2 and 3, respectively. CSD nos. 416726 for **1** and 416727 for **2**.

3. Results and discussion

3.1. Thermal properties

The TGA experiment for **1** showed a weight loss of ca. 1.6% in the temperature range 323–400 K, which presumably was associated with the removal of physically absorbed water. The reason for another mass loss of ca. 2.0% in the range of 400–1060 K might be associated with the loss of boron (Fig. 1). In order to establish exactly the thermal behavior of **1**, a thermodiffractometry in air was performed between 300 and 1073 K with a step interval of 100 K. The result showed that the phase observed at room temperature was retained until 973 K with decreased crystallinity and transformed into amorphous glassy state at 1073 K. The thermal expansion of **1** in the low- and high-temperature region is approximately isotropic as shown in Fig. 2 and slightly pronounced along

Table 1
Crystallographic data and refinement parameters for $Na_3B_6PO_{13}$ and $Na_3BP_2O_8$

Structural parameters	**1**	**2**
Empirical formula	$Na_3B_6PO_{13}$	$Na_3BP_2O_8$
Formula weight	372.8	269.7
Wavelength	Mo$K\alpha$ (0.71073 Å)	Mo$K\alpha$ (0.71073 Å)
Crystal system, space group	Orthorhombic, *Pnma* (no. 62)	Monoclinic, *C*2/*c* (no. 15)
Unit cell dimensions	$a = 9.3727(4)$ Å	$a = 12.567(4)$ Å
	$b = 16.2307(7)$ Å	$b = 10.290(3)$ Å, $\beta = 92.492(5)^\circ$
	$c = 6.7232(3)$ Å	$c = 10.210(3)$ Å
Volume	1022.77(8) Å^3	1319.1(7) Å^3
Z, calculated density	4, 2.42 g/cm^3	8, 2.72 g/cm^3
Abs coeff, μ(Mo$K\alpha$), (mm^{-1})	0.477	0.870
Theta range for data collection	3.28–27.47°	2.56–27.00°
Reflections collected/unique	1203/881 [$R_{int} = 0.0275$]	1434/1109 [$R_{int} = 0.0259$]
Goodness-of-fit on F^2	1.081	0.913
Final *R* indices [$I > 2\sigma(I)$]	$R_1 = 0.0358$[a], w$R_2 = 0.0978$[b]	$R_1 = 0.0303$[a], w$R_2 = 0.0675$[b]
R indices (all data)	$R_1 = 0.0509$, w$R_2 = 0.1092$	$R_1 = 0.0401$, w$R_2 = 0.0697$
Largest diff. peak and hole	−0.59 and 0.35	−0.51 and 0.40

[a] $R_1 = \Sigma \| F_o | - | F_c \| / \Sigma | F_o |$.
[b] $wR_2 = \{\Sigma[w(F_o^2 - F_c^2)^2] / \Sigma[w(F_o^2)^2]\}^{1/2}$.

Table 2
Selected bond lengths (Å) and angles (deg.) for $Na_3B_6PO_{13}$[a]

P(1)–O(3)	1.486(2)	Na(1)–O(1)#6	2.355(2)
P(1)–O(1)	1.491(2)	Na(1)–O(8)#7	2.457(2)
P(1)–O(2)	1.578(2)	Na(1)–O(4)#8	2.519(2)
P(1)–O(2)#1	1.578(2)	Na(1)–O(4)#9	2.519(2)
B(1)–O(2)	1.480(3)	Na(1)–O(8)#9	2.530(2)
B(1)–O(4)	1.489(3)	Na(1)–O(7)#7	2.573(2)
B(1)–O(7)	1.496(3)	Na(1)–O(7)#10	2.573(2)
B(1)–O(8)	1.414(3)	Na(2)–O(2)#11	2.455(2)
B(2)–O(4)	1.336(3)	Na(2)–O(2)#5	2.485(2)
B(2)–O(5)	1.382(2)	Na(2)–O(1)#5	2.510(2)
B(2)–O(6)#15	1.382(3)	Na(2)–O(3)#11	2.510(2)
B(3)–O(5)	1.386(2)	Na(2)–O(7)#5	2.548(2)
B(3)–O(6)	1.379(2)	Na(2)–O(6)	2.605(2)
B(3)–O(7)	1.343(3)	Na(2)–O(5)#12	2.638(2)
Na(1)–O(3)	2.350(2)	Na(2)–O(4)#11	2.662(2)
O(3)–P(1)–O(1)	119.48(11)	O(8)–B(1)–O(7)	109.77(16)
O(3)–P(1)–O(2)	107.70(5)	O(2)–B(1)–O(7)	106.94(16)
O(1)–P(1)–O(2)	107.87(5)	O(4)–B(1)–O(7)	109.17(14)
O(3)–P(1)–O(2)#1	107.70(5)	O(4)–B(2)–O(5)	123.16(19)
O(1)–P(1)–O(2)#1	107.87(5)	O(4)–B(2)–O(6)#5	121.95(19)
O(2)–P(1)–O(2)#1	105.38(8)	O(5)–B(2)–O(6)#5	114.83(15)
O(8)–B(1)–O(2)	113.24(18)	O(7)–B(3)–O(6)	120.79(19)
O(8)–B(1)–O(4)	110.63(16)	O(7)–B(3)–O(5)	121.93(19)
O(2)–B(1)–O(4)	106.93(16)	O(6)–B(3)–O(5)	117.27(15)

Bond valence sums (Σs): [P(1)O_4] tetrahedron, Σs[P(1)−O] = 4.88; [B(1)O_4] tetrahedron, Σs[B(1)−O] = 3.08; [B(2)O_3] triangle, Σs[B(2)−O] = 3.04; [B(3)O_3] triangle, Σs[B(3)−O] = 3.02; [Na(1)O_8], Σs[Na(1)−O] = 1.30 [Na(2)O_8], Σs[Na(2)−O] = 1.08.

[a] Symmetry transformations used to generate equivalent atoms: (#1) *x*, 0.5−*y*, *z*; (#2) 0.5−*x*, 1−*y*, −0.5+*z*; (#3) 0.5−*x*, −0.5+*y*, −0.5+*z*; (#4) −*x*, −0.5+*y*, 1−*z*; (#5) −*x*, 1−*y*, 1−*z*; (#6) 0.5+*x*, *y*, −0.5−*z*; (#7) 0.5+*x*, *y*, 0.5−*z*; (#8) *x*, 0.5−*y*, −1+*z*; (#9) *x*, *y*, −1+*z*; (#10) 0.5+*x*, 0.5−*y*, 0.5−*z*; (#11) 0.5−*x*, 1−*y*, 0.5+*z*; (#12) −0.5+*x*, *y*, 1.5−*z*; (#13) −0.5+*x*, *y*, −0.5−*z*; (#14) *x*, *y*, 1+*z*; (#15) 0.5+*x*, *y*, 1.5−*z*; (#16) −0.5+*x*, *y*, 0.5−*z*.

Table 3
Selected bond lengths (Å) and angles (deg.) for $Na_3BP_2O_8$[a]

P(1)–O(4)	1.490(3)	Na(2)–O(8)#10	2.285(2)
P(1)–O(2)	1.503(2)	Na(2)–O(6)	2.307(2)
P(1)–O(3)	1.586(2)	Na(2)–O(2)	2.314(2)
P(1)–O(1)	1.587(3)	Na(2)–O(6)#4	2.474(3)
P(2)–O(8)	1.499(3)	Na(2)–O(4)	2.905(3)
P(2)–O(6)	1.503(3)	Na(3)–O(2)#4	2.245(4)
P(2)–O(7)	1.577(2)	Na(3)–O(2)	2.245(4)
P(2)–O(5)	1.582(2)	Na(3)–O(1)#1	2.461(3)
B(1)–O(7)#5	1.460(5)	Na(3)–O(1)#8	2.461(3)
B(1)–O(1)	1.465(5)	Na(3)–O(3)#1	2.470(6)
B(1)–O(5)#4	1.468(4)	Na(3)–O(3)#8	2.470(6)
B(1)–O(3)#1	1.503(4)	Na(4)–O(4)#12	2.390(5)
Na(1)–O(4)#6	2.288(4)	Na(4)–O(4)	2.390(5)
Na(1)–O(5)	2.455(5)	Na(4)–O(8)#4	2.405(6)
Na(1)–O(2)	2.483(6)	Na(4)–O(8)#13	2.405(6)
Na(1)–O(8)#7	2.490(6)	Na(4)–O(6)#11	2.666(3)
Na(1)–O(3)#8	2.600(6)	Na(4)–O(6)#10	2.666(3)
Na(1)–O(7)#9	2.612(2)	Na(4)–O(1)#12	2.902(3)
Na(1)–O(6)#9	2.616(3)	Na(4)–O(1)	2.902(3)
O(4)–P(1)–O(2)	114.48(11)	O(8)–P(2)–O(5)	111.24(10)
O(4)–P(1)–O(3)	110.32(10)	O(6)–P(2)–O(5)	107.58(10)
O(2)–P(1)–O(3)	110.97(10)	O(7)–P(2)–O(5)	104.38(10)
O(4)–P(1)–O(1)	107.47(10)	O(7)#5–B(1)–O(1)	106.60(19)
O(2)–P(1)–O(1)	111.76(10)	O(7)#5–B(1)–O(5)#4	113.57(22)
O(3)–P(1)–O(1)	100.95(9)	O(1)–B(1)–O(5)#4	112.35(21)
O(8)–P(2)–O(6)	115.61(11)	O(7)#5–B(1)–O(3)	108.96(21)
O(8)–P(2)–O(7)	111.28(10)	O(1)–B(1)vO(3)	112.80(21)
O(6)–P(2)–O(7)	106.02(10)	O(5)#4–B(1)–O(3)	102.65(21)

Bond valence sums (Σs): [P(1)O_4] tetrahedron, Σs[P(1)−O] = 4.77; [P(2)O_4] tetrahedron, Σs[P(2)−O] = 4.77; [B(1)O_4] tetrahedron, Σs[B(1)−O] = 3.03; [Na(1)O_7], Σs[Na(1)−O] = 1.08; [Na(2)O_5], Σs[Na(2)−O] = 0.99; [Na(3)O_6], Σs[Na(1)−O] = 1.26; [Na(4)O_8], Σs[Na(2)−O] = 1.09.

[a] S*y*mmetr*y* transformations used to generate equivalent atoms: (#1) −*x*, 2−*y*, 2−*z*; (#2) 0.5−*x*, −0.5+*y*, 1.5−*z*; (#3) *x*, 1−*y*, −0.5+*z*; (#4) −*x*, *y*, 1.5−*z*; (#5) −0.5+*x*, 1.5−*y*, 0.5+*z*; (#6) 0.5−*x*, 1.5−*y*, 2−*z*; (#7) 0.5−*x*, 1.5−*y*, 1−*z*; (#8) *x*, 2−*y*, −0.5+*z*; (#9) 0.5−*x*, 0.5+*y*, 1.5−*z*; (#10) *x*, 1−*y*, 0.5+*z*; (#11) −*x*, 1−*y*, 2−*z*; (#12) −*x*, *y*, 2.5−*z*; (#13) *x*, *y*, 1+*z*; (#14) *x*, 2−*y*, 0.5+*z*; (#15) 0.5+*x*, 1.5−*y*, −0.5+*z*; (#16) *x*, *y*, −1+*z*.v.

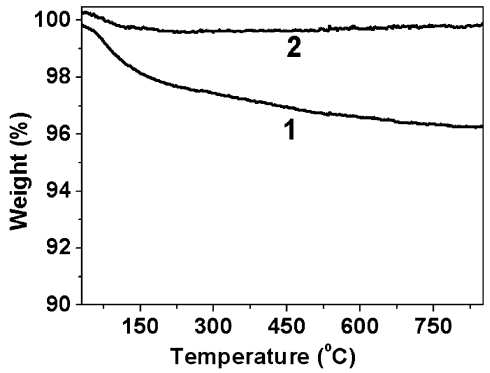

Fig. 1. The TG curves for $Na_3B_6PO_{13}$ (1) and $Na_3BP_2O_8$ (2).

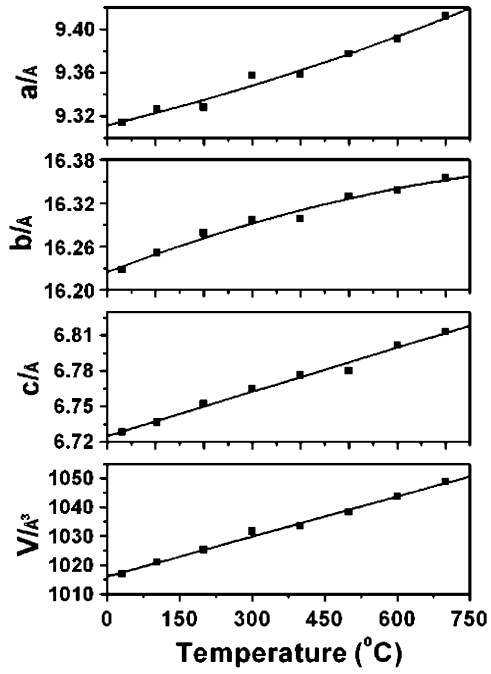

Fig. 2. Changes of lattice parameters as a function of temperature for $Na_3B_6PO_{13}$, $a(T)$, $b(T)$, $c(T)$ and $V(T)$. The drawn line are polynomial fits of second order for $a(T)$ and $b(T)$, and first order for $c(T)$ and $V(T)$, respectively: $a(T) = 9.31166 + 1.06301 \times 10^{-4}\,T/K + 4.96207 \times 10^{-8}\,T^2/K^2$, $b(T) = 16.22462 + 2.56835 \times 10^{-4}\,T/K - 1.07036 \times 10^{-7}\,T^2/K^2$, $c(T) = 6.725 + 1.24491 \times 10^{-4}\,T/\mathrm{K}$ and $V(T) = 1016.03016 + 0.04614\,T/K$.

the *b*-axis direction. A linear behavior is observed for the *c*-axis in the whole temperature range, while second order as a function of temperature for *a*- and *b*-axis. Lattice parameters between 300 and 973 K have been determined by indexing using TREOR module in the STOE software package.

The TGA analysis for **2** showed almost no weight loss in the temperature range of 300–1123 K besides the marginal elimination of physically absorbed water (ca. 0.35%) before 420 K (Fig. 1). After thermal treated, glassy residue was also observed in **2**, and X-ray powder diffraction confirmed it was amorphous.

3.2. IR spectroscopy

The infrared (IR) spectra of **1** contained several high-frequency peaks at 1540, 1447 and 1384 cm^{-1}: these are related to the stretching vibrations of the triangular BO_3 [11]. The bands in the region, 1180–476 cm^{-1} and 1236–497 cm^{-1} in **1** and **2**, respectively, can be assigned to the asymmetric stretching and bending vibrations of PO_4, BO_4 and B–O–P groups [12,13]. The stretching bands of the OH at ca. 3700–3300 cm^{-1}(broad) contributed by physically absorbed water in the spectra of **1** and **2**.

3.3. $Na_3B_6PO_{13}$: crystal structure and characterization

The asymmetric unit in the structure of **1** consists of two crystallographically distinct trigonal planar coordinated B sites, one tetrahedrally coordinated B site, one tetrahedrally coordinated P site, two Na atoms, eight oxygen atoms. The B–O distances and O–B–O angles are varying from 1.336(3) to 1.496(3) Å and 106.93(16) to 123.16(19)° (averges of 119.99(18)° in trigonally coordinated B and 109.45(16)° in tetrahedrally), respectively. For the phosphate groups P–O distances and O–P–O angles cover the ranges from 1.486(2) to 1.578(2) Å and 105.38(8) to 119.48(11)° (averge of 109.33(6)°), respectively. The crystal structure of the compound contains complex anions $^1_\infty\{[B_6PO_{13}]\}^{3-}$ built of BO_3, BO_4 and PO_4 polyhedra linked via common vertexes that are arranged parallel to [100]. Adjacent chains $^1_\infty\{[B_6PO_{13}]\}^{3-}$ insert into each other forming corrugated layers parallel to *ac*. The sodium ions are located in the central positions of the chain as well as in the voids between the chains (Fig. 3). On the basis of bond strength calculations [14,15], the bond valences sums for Na, P, and B atoms are close to their formal valences of 1, 5, and 3, respectively, which indicates proper assignment of the anion groups (listed in Table 2).

Compound **1** and $KB_6PO_{10}(OH)_4$ [4b] are the two borophosphates with the highest borate content found so far with the same molar ratio B:P = 6:1. However, as shown in Fig. 4, the chemical differences cause major differences in the configurations of fundamental building units (FBU). In compound **1**, FBU can be described as B_6PO_{15} (noted as $\Delta|\Delta|\Delta$) consisting of two borate three-membered rings (Δ) connected by borate–phosphate three-membered ring (Δ) through vertexes. In other words, two three-membered rings built of two BO_3 groups and one BO_4 group link to each other via common vertexes in BO_4, and the two connected BO_4 share their remaining corners with single loop branching PO_4 group with two terminal oxygen atoms (P = O1 = 1.491(2) Å and P = O3 = 1.486(2) Å). Linkage of these FBUs to each other via common vertexes in BO_3 in an alternating fashion with opposite orientations forms the backbone of the chain containing an eight-membered ring (size in 7.731 × 4.986 Å) built exclusively of BO_3 and BO_4 groups (Fig. 4b–c). In $KB_6PO_{10}(OH)_4$, FBUs are defined as $B_6PO_{12}(OH)_4$ (noted as $\Delta|<|\Delta$) consisting of two borate

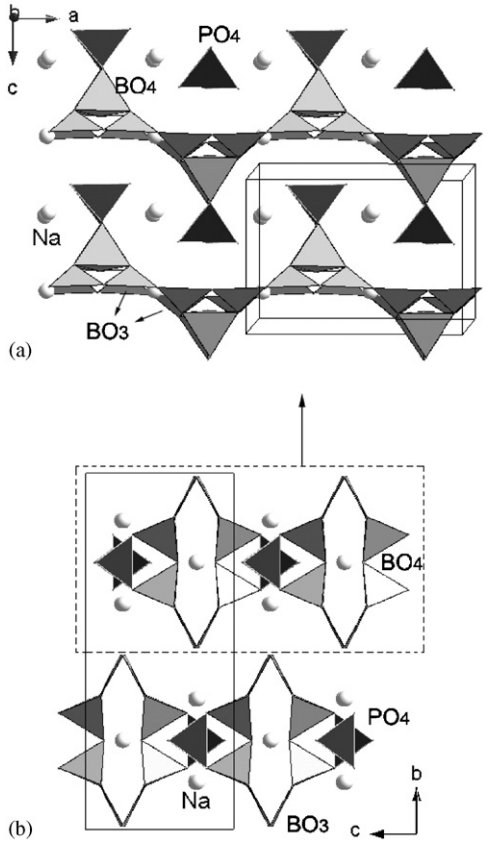

Fig. 3. Representation of crystal structure and cation positions in $Na_3B_6PO_{13}$: (a) the neighboring chains insert into each other in single-layer, and (b) borophosphate chains are arranged parallel to [100]. 8-fold coordinated Na atoms are located in the channels and the spaces between the chains. For clarity, the Na–O bonds are not connected. Dark tetrahedra: PO_4; gray tetrahedra: BO_3 and BO_4; gray sphere: sodium atom.

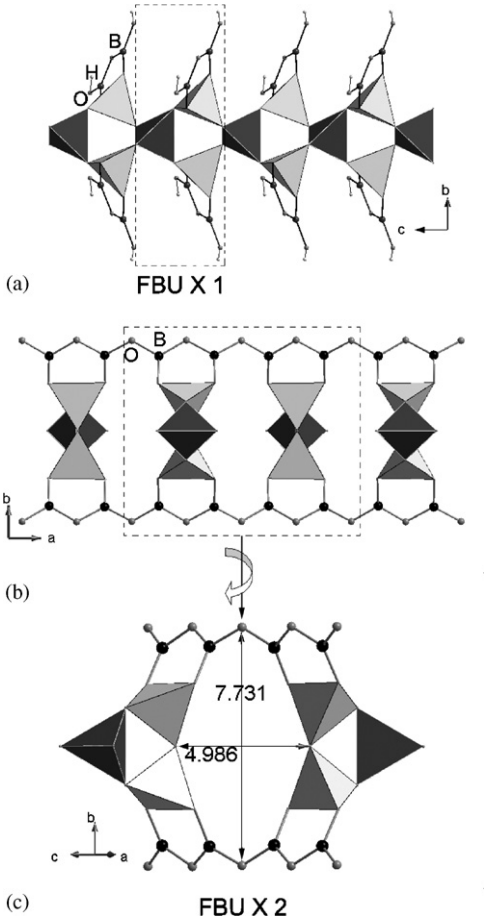

Fig. 4. Representation of the fundamental building unit (FBU): (a) $[B_6PO_{12}(OH)_4]$ in $K[B_6PO_{10}(OH)_4]$, (b) $[B_6PO_{15}]$ in $Na_3B_6PO_{13}$ and (c) two FBUs form an eight-membered ring (size in 7.731×4.986 Å). Infinite sequence of these FBUs form the two different chains as the way showed in figure. Dark tetrahedra: PO_4; gray tetrahedra: BO_4, gray sphere: oxygen atom; smaller gray sphere: hydrogen atom; black sphere: boron atom.

3-rings (Δ) linked by one tetrahedral phosphate ($<$) through vertexes, and connected to each other as the way shown in Fig. 4a.

Besides the significant differences in cation sizes (eight-fold coordination: $r_{ef} \approx (Na^+) 1.18$ Å; $r_{ef}(K^+) \approx 1.51$ Å) [16], the difference in structural arrangement mentioned above might be ascribed to the protonation of the BO_3 and formation of $BO_2(OH)$ in $KB_6PO_{10}(OH)_4$. Firstly, the protonated BO_3 gives rise to the lower number of cations. Secondly, the formation of hydrogen bonds also influences the structure. At last, the protonated BO_3 does not contribute to interconnection, which is regarded as a possible explanation for the fact that no borophosphate of higher dimensionality have been found for B:P > 1:1 [4a]. Whether or not the anions are protonated is probably due to their synthetic conditions, compound **1** by flux method while $KB_6PO_{10}(OH)_4$ by hydrothermal method. It is apt in forming anhydrous instead of hydrated borate group in the environment of water-free or trace water (from reaction) in low-temperature flux method. If one focuses on the synthetic conditions of borophosphates, the majority of borophosphates prepared by hydrothermal method are hydrated phases with the several exceptional examples, such as $Sr[BPO_5]$ [1a] and $Na_5[B_2P_3O_{10}]$ [4e], but all borophosphates prepared by flux method are anhydrous phases to date [8a,9].

3.4. *$Na_3BP_2O_8$: crystal structure and characterization*

The asymmetric unit in the structure of **2** consists of one crystallographically distinct tetrahedrally coordinated B site, two tetrahedrally coordinated P site, four Na atoms and eight oxygen atoms. The B–O distances and O–B–O angles vary from 1.460(5) to 1.503(4) Å and 102.65(21) to 113.57(22)° (averge of 109.49(21)°), respectively. For the phosphate groups, P–O distances and O–P–O angles cover the ranges from 1.490(3) to 1.587(3) Å and 100.95(9) to 115.61(11)° (averge of 109.34(10)°), respectively. The condensation of BO_4 and PO_4 tetrahedra through common vertexes leads to straight anionic chains of $^1_\infty\{[BP_2O_8]\}^{3-}$. The infinite straight chains are built of four-membered rings of tetrahedra in which the BO_4 and PO_4 groups

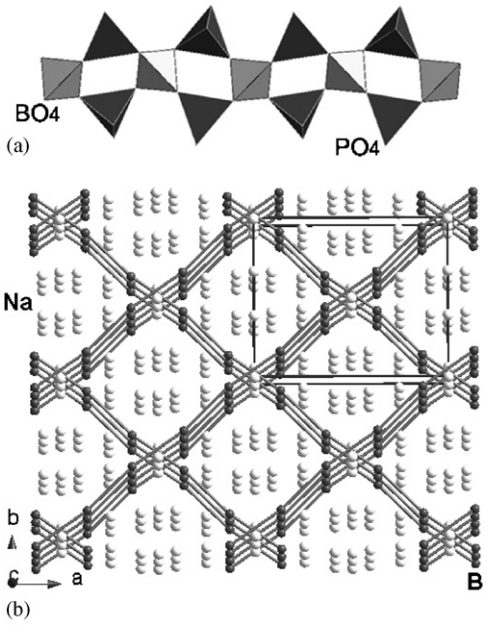

Fig. 5. The straight chains in $Na_3BP_2O_8$: (a) The infinite chain built of four-membered rings of the tetrahedral along the central borate chain, in which all vertexes of the BO_4 groups participate in bridging functions with PO_4 tetrahedra, (b) The chains across to each other in neighboring layers. The chain of boron atoms represents the borophosphate chain for clarity. Na ions are located in the voids.

alternate. Each BO_4 tetrahedra is joined to the adjacent four-membered rings of PO_4 tetrahedra along the chain in such a way that all vertexes of the BO_4 groups participate in bridging functions with PO_4 tetrahedra. The phosphate groups occupy the borders of the chains with two terminal oxygen atoms (Fig. 5a). Compared with previously reported borophosphate with a molar ratio B:P = 1:2, The infinite four-membered ring connectivity in **2** is not found in other alkali metal borophosphates to date, but analogous straight one is found in $Cs(ZnBP_2O_8)$ [1e] and $NH_4(Zn_{0.88}Co_{0.12}BP_2O_8)$ [5], and helical one in the $(C_4N_3H_{16})[Zn_3B_3P_6O_{24}]\cdot H_2O$ [1d] and $M^IM^{II}(H_2O)_2[BP_2O_8]\cdot H_2O$ (M^I = Li, Na, K, NH_4; M^{II} = Mg, Mn, Fe, Co, Ni, Zn, Cd) [1i,1j]. Dissimilar to $Cs(ZnBP_2O_8)$ and $NH_4(Zn_{0.88}Co_{0.12}BP_2O_8)$ in which all straight chains parallel to each other, straight chains in **2** have different directions. The chains parallel to each other in one monolayer, and the chains rotate by about 100° related to the chains in the neighboring layer, which is a unique feature (Fig. 5b). According to the directions of chains, we can defined **2** as a layered-structure compound with a repeating arrangement of AB⋯AB layers along the *c*-axis.

The sodium ions reside between chains compensate the negative charges of borophosphate chains and hold the layers together into the 3-D structure through bonding with oxygen atoms of chains (Fig. 6). Na(1), Na(2), Na(3) and Na(4) are 7-, 5-, 6- and 8-fold coordinated, respectively. Bond strength calculations were also carried out for **2** and the bond valences sums for Na, P, and B atoms are close to their formal valences of 1, 5, and 3 too.

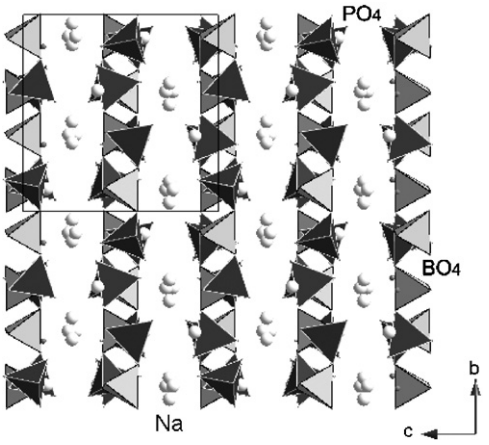

Fig. 6. Representation of crystal structure and cation positions in $Na_3BP_2O_8$. 5-, 6-, 7- and 8-fold coordinated Na atoms are located between the chains. The Na–O bonds are not connected for clarity.

4. Conclusion

In summary, two anhydrous borophosphates with 1-D structures, $Na_3B_6PO_{13}$ and $Na_3BP_2O_8$, was prepared by low-temperature molten salt method using boric acid and sodium dihydrogen phosphate as fluxes respectively. $Na_3B_6PO_{13}$ shows an infinite chain of $^1_\infty\{[BP_6O_{13}]\}^{3-}$ containing eight-membered ring in which all vertexes of borate group contribute to interconnection. $Na_3BP_2O_8$ reveals an infinite straight chain of $^1_\infty\{[BP_2O_8]\}^{3-}$ built of vertexes-sharing four-membered rings, and chains in neighboring layers arranged along different orientations.

The low-temperature molten salt method is further proven to be an efficient supplemental tool to synthesize new borophosphates, especially anhydrous phases in mild temperature. These anhydrous borophosphates consist of some new anionic structural units, such as eight-membered ring built exclusively of borate groups in $Na_3B_6PO_{13}$. And the known building unit is extended to other systems with new arrangement in $Na_3BP_2O_8$. As shown in the examples of $Na_3B_6PO_{13}$ (excess H_3BO_3 in starting reactants) with B:P = 6, NH_4BPO_4F (the amount of H_3BO_3 equal to that of phosphate in starting reactants) with B:P = 1 and $Na_3BP_2O_8$ (excess phosphate in starting reactants) with B:P = 0.5, the possibility of changing the number of B–O–P bonds by adjusting the ratio of B:P in starting reactants is another advantage for the technique.

Acknowledgments

This work was supported by the Key Project (50332050) from the NNSF of China and the Hundred Talents Program from the Chinese Academy of Sciences and fund for Young Leading Researchers from Shanghai municipal government. The authors wish to thank Ying-Jie Zhu's research group for their great help in measuring TG-DSC. Helpful discussions with Professor Huang Fu-Qiang are also greatly acknowledged.

Appendix A. Supplementary materials

CCDC 〈data_b and data_bp2〉 contains the supplementary crystallographic data for 〈SHELXL-97〉. These data can be obtained free of charge via http://www.ccdc.cam.ac.uk/conts/retrieving.html, or from the Cambridge Crystallographic Data Centre, 12 Union Road, Cambridge CB2 1EZ, UK; fax: (+44) 1223-336-033; or e-mail: deposit@ccdc.cam.ac.uk.

Appendix B. Supplementary materials

Supplementary data associated with this article can be found in the online version at doi:10.1016/j.jssc.2006.09.034

References

[1] [a] R. Kniep, G. Gözel, B. Eisenmann, C. Röhr, M. Asbrand, M. Kizilyalli, Angew. Chem. Int. Ed. 33 (1994) 749–751;
[b] S.C. Sevov, Angew. Chem. Int. Ed. 35 (1996) 2630–2632;
[c] R. Bontchev, J. Do, A.J. Jacobson, Angew. Chem. Int. Ed. 38 (1999) 1937–1940;
[d] W. Liu, M.R. Li, H.H. Chen, X.X. Yang, J.T. Zhao, Dalton Trans. (2004) 2847–2849;
[e] R. Kniep, G. Schäfer, H. Engellhardt, I. Boy, Angew. Chem. Int. Ed. 38 (1999) 3642–3644;
[f] Y.X. Huang, G. Schäfer, W. Carrillo-Cabrera, R. Cardoso, W. Schnelle, J.T. Zhao, R. Kniep, Chem. Mater. 13 (2001) 4348–4354;
[g] E. Dumas, C. Debiemme-Chouvy, S.C. Sevov, J. Am. Chem. Soc. 124 (2002) 908–909;
[h] W. Liu, M.H. Ge, X.X. Yang, H.H. Chen, M.R. Li, J.T. Zhao, Inorg. Chem. 43 (2004) 3910–3914;
[i] R. Kniep, H.G. Will, I. Boy, C. Röhr, Angew. Chem. Int. Ed. 36 (1997) 1013–1014;
[j] M.H. Ge, J.X. Mi, Y.X. Huang, J.T. Zhao, R. Kniep, Kristallogr. NCS 218 (2003) 165–166;
[k] I. Boy, G. Cordier, R. Kniep, Z. Kristallogr. New Cryst. Struct. 213 (1998) 29–30;
[l] R. Kniep, G. Schäfer, Z. Anorg. Allg. Chem. 626 (2000) 141;
[m] C. Hauf, R. Kniep, Z. Naturforsch. 52b (1997) 1432–1435.

[2] F. Liebau, Structural Chemistry of Silicates, Springer, Heidelberg, 1985.

[3] R. Kniep, H. Engelhardt, C. Hauf, Chem. Mater. 10 (1998) 2930–2934.

[4] [a] B. Ewald, Y. Prots, P. Menezes, S. Natarajan, H. Zhang, R. Kniep, Inorg. Chem. 44 (2005) 6431–6438;
[b] I. Boy, R. Kniep, Z. Naturforsch. B 54 (1999) 895–898;
[c] C. Hauf, R. Kniep, Z. Kristallogr. New Cryst. Struct. 211 (1996) 707–708;
[d] C. Hauf, R. Kniep, Z. Kristallogr. New Cryst. Struct. 212 (1997) 313–314;
[e] C. Hauf, T. Friedrich, R. Kniep, Z. Kristallogr. New Cryst. Struct. 210 (1995) 446;
[f] C. Hauf, R. Kniep, Z. Naturforsch. B 52 (1997) 1432–1435;
[g] R. Kniep, H.Z. Engelhardt, Anorg. Allg. Chem. 624 (1998) 1291–1297.

[5] G. Schäfer, H. Borrmann, R. Kniep, Micropor. Mesopor. Mater. 41 (2000) 161–167.

[6] [a] P.C. Lu, Y.X. Wang, J.H. Lin, L.P. You, Chem. Commun. (2001) 1178–1179;
[b] J. Ju, J.H. Lin, G.B. Li, T. Yang, H.M. Li, F.H. Liao, C.K. Loong, L.P. You, Angew. Chem. Int. Ed. 42 (2003) 5607–5610;
[c] L.Y. Li, G.B. Li, Y.X. Wang, F.H. Liao, J.H. Lin, Chem. Mater. 17 (2005) 4174–4180;
[d] L.Y. Li, X.L. Jin, G.B. Li, Y.X. Wang, F.H. Liao, G.Q. Yao, J.H. Lin, Chem. Mater. 15 (2003) 2253–2260;
[e] L.Y. Li, P.C. Lu, Y.Y. Wang, X.L. Jin, G.B. Li, Y.X. Wang, L.P. You, J.H. Lin, Chem. Mater. 14 (2002) 4963–4968.

[7] [a] I.D. Williams, M.M. Wu, H.H.Y. Sung, X.X. Zhang, J.H. Yu, Chem. Commun. (1998) 2463–2464;
[b] H.H.Y. Sung, M.M. Wu, I.D. Williams, Inorg. Chem. Commun. 3 (2000) 401–404.

[8] [a] M.R. Li, W. Liu, M.H. Ge, H.H. Chen, X.X. Yang, J.T. Zhao, Chem. Commun. (2004) 1270–1272;
[b] W. Liu, M.R. Li, H.H. Chen, X.X. Yang, J.T. Zhao, J. Solid State Chem. 178 (2005) 912–916.

[9] M. Yang, J.H. Yu, P. Chen, J.Y. Li, Q.R. Fang, R.R. Xu, Micropor. Mesopor. Mater. 87 (2005) 124–132.

[10] [a] R.H. Blessing, Acta Crystallogr. Sect. A. 51 (1995) 33;
[b] SADABS, Area-Detector Absorption Correction, Bruker-AXS, Madison, WI, 1996;
[c] G.M. Sheldrick, SHELXTL Programs, Release Version 5.1, Bruker-AXS, Madison, WI, 1998.

[11] Y. Shi, J.K. Liang, H. Zhang, J.L. Yang, W.D. Zhuang, G.H. Rao, J. Solid State Chem. 129 (1997) 45–52.

[12] Y. Shi, J.K. Liang, H. Zhang, Q.L. Liu, X.L. Chen, J.L. Yang, W.D. Zhuang, G.H. Rao, J. Solid State Chem. 135 (1998) 43–51.

[13] A. Baykal, M. Kizilyalli, R. Kniep, J. Mater. Sci. 35 (2004) 4621–4626.

[14] N.E. Brese, M. O'Keefe, Acta Crystallogr. B 47 (1991) 192–197.

[15] I.D. Brown, Acta Crystallogr. B 48 (1992) 553–572.

[16] J.K. Liang, Crystal Structure Determination from Powder Diffraction Data, Science Press, Moscow, 2003, pp. 131–148 (in Chinese).